regions are smaller, the positioning accuracy is better.

7. Conclusions

In this paper, we analyze the propagation of UWB signals inside of human body tissues with the FDTD method. Especially, we focused on the time-based position estimation of medical implanted devices inside human body. Firstly, we apply an adaptive template synthesis method in multipath channel for calculate the propagation time accurately based on the output of the correlator between the transmitter and the receiver. Furthermore, we analyze the relative permittivity of human homogeneous tissues. In addition, we analyze the relationship between the RMSE of position estimation and bandwidth of UWB signals. As a result, we show that UWB signals of 4 GHz bandwidth have a beneficial effect on the position estimation of medical implanted devices.

Moreover, we have proposed the position estimation method of medical implanted devices using estimation of the propagation velocity inside of the human body. Simulation results show that the proposed method gives a positioning accuracy around the size of medical implanted devices such as capsule endoscopes. In addition, simulation results show that if the regions are smaller, the positioning accuracy is better.

In the future, we estimate the propagation velocity inside human body without prior information of human body images. Furthermore, we expand our 2D model inside human body to 3D model. In 3D model analysis, we additionally need to consider the more complex structure of human body tissues. So the signals refract at the boundary of tissues many times. So we need to estimate so precisely the increase of propagation time based on the refractions of the signal.

References

[1] M.Z. Win and R.A. Scholtz, "Ultra-wide bandwidth time-hopping spread-spectrum impulse radio for wireless multiple-access communications," IEEE Trans. Commun., vol.48, no.4, pp.679–691, April 2000.

[2] S. Gezici, Z. Tian, G.B. Giannakis, H. Kobayashi, A.F. Molisch, H.V. Poor, and Z. Sahinoglu, "Localization via ultra wideband radios," IEEE Signal Process. Mag., vol.22, no.4, pp.70–84, July 2005.

[3] A.H. Sayed, A. Tarighat, and N. Khajehnouri, "Network-based wireless location," IEEE Signal Process. Mag., vol.22, no.4, pp.24–40, July 2005.

[4] K. Taniguchi and R. Kohno, "Design and analysis of synthesized template waveform for receiving UWB signals," IEICE Trans., Fundamentals, vol.E88-A, no.9, pp.2299–2309, Sept. 2005.

[5] G. Sun and C.W. Trueman, "Numerical dispersion and numerical loss in finite-difference time-domain method in lossy media," IEEE Trans. Antennas Propag., vol.53, no.11, pp.3684–3690, Nov. 2005.

[6] K. Tai, H. Harada, and R. Kohno, "Channel modeling and signaling of medical implanted communication systems and a step to medical ICT," A3.5, IST Mobile Summit 2007, July 2007.

[7] A. Alomainy, Y. Hao, Y. Yuan, and Y. Liu, "Modelling and characterisation of radio propagation from wireless implants at different frequencies," Proc. 9th European Conference on Wireless Technology, pp.119–122, Sept. 2006.

[8] T. Nakamura, M. Shimizu, H. Kimura, and R. Sato, "Effective permittivity of amorphous mixed materials," IEICE Trans. Commun. (Japanese Edition), vol.J87-B, no.11, pp.1951–1958, Nov. 2004.

[9] M. Kawasaki, H. Harada, and R. Kohno, "Position estimation method of medical implanted devices using estimation of propagation velocity inside human body," Proc. ISMICT'07, Oulu, Finland, Dec. 2007.

Makoto Kawasaki received the Bachelor of Engineering degree in electrical and computer engineering form Yokohama National University, Yokohama, Japan, in 2007. He is currently working toward the M.S. degree in electrical and computer engineering form Yokohama National University, Yokohama, Japan. His research interests lie in the area of medical information and communications technologies.

Ryuji Kohno received the B.E. and M.E. degrees in computer engineering form Yokohama National University in 1979 and 1981 respectively and the Ph.D. degree in electrical engineering from the University of Tokyo in 1984. He has been a Professor of the Division of Electrical and Computer Engineering, Yokohama National University (YNU) since 1998. He was a director of SONY Advanced Telecommunications Laboratory during 1998–2002 and a director of UWB Technology institute of National Institute of Information and Communications Technology (NICT), and a President of 21st century COE (Center of Excellence) of Creation of Future Social Infrastructure Based on Information Telecommunications Technology in YNU during 2002–2007. Currently, he is a director of the Medical Information and Communication Technology Center in Yokohama National University as well as a director of the Medical ICT institute of the NICT. He was covering a wide area of information theory and its application such as coding theory, spread spectrum system, space-time coding and signal processing, SDR (Software Defined Radio), UWB (Ultra Wide-Band), and their applications to medical care, intelligent transport system (ITS) and so on. Prof. Kohno was elected to be a member of the Board of Governors of IEEE Information Theory Society twice on 2000 and 2003. He was an editor of the IEEE Transactions on Information Theory during 1995–1998, currently is that of the IEEE Transactions on Communications since 1994, and that of IEEE Transactions on Intelligent Transport Systems (ITS) since 2000. He has been a vice-president of Engineering Sciences Society of IEICE, the Chairman of the IEICE Technical Committee on Spread Spectrum Technology, that on ITS and that on SDR. Currently he is an editor in cheif of the IEICE Transactions on Fundamentals of Electronics, Communications, and Computer Sciences, and the vice-president of SITA(Society of Information Theory and its Applications). He was awarded IEICE Greatest Contribution Award and NTT DoCoMo Mobile Science Award in 1999 and 2002, respectively.

A TOA based Positioning Technique of Medical Implanted Devices

Makoto Kawasaki, Ryuji Kohno

Division of Physics, Electrical and Computer Engineering, Yokohama National University
79-5 Tokiwadai, Hodogaya, Yokohama, 240-8501, Japan
Tel: +81-45-339-4116, Fax: +81-45-338-1176
E-mail: makoto@kohnolab.dnj.ynu.ac.jp,kohno@ynu.ac.jp

Abstract

Wireless communication devices in the field of medical implant, such as cardiac pacemakers and capsule endoscopes, have been studied and developed to improve healthcare systems. Especially it is very important to know the range and position of each device because it will contribute to an optimization of the transmission power. We adopt the time-based approach of position estimation using ultra wideband signals. However, the propagation velocity inside the human body differs in each tissue and each frequency. Furthermore, the human body is formed of various tissues with complex structures. For this reason, propagation velocity is different at a different point inside human body and the received signal so distorted through the channel inside human body. In this paper, we apply an adaptive template synthesis method in multipath channel for calculate the propagation time accurately based on the output of the correlator between the transmitter and the receiver. Furthermore, we propose a position estimation method using an estimation of the propagation velocity inside the human body. In addition, we show by computer simulation that the proposal method perform accurate positioning with a size of medical implanted devices such as a medicine capsule.

Keywords: medical implanted device, position estimation, ultra wideband, propagation velocity

Ⅰ. Introduction

Recently, wireless communication devices in the field of medical implant (cardiac pacemaker and capsule endoscope and so on) are studied extensively towards practical use. In the future, by transmitting vital data from one device to another implanted device in a network of medical implants, we can observe the body's condition and to detect any possible problem in the human body at anytime and anywhere. These can be a great help for doctors to diagnose and to cure diseases[4].

Considering that transmitted information of vital data is highly important and the need for long-lasting batteries, it is important that wireless communications of medical implanted devices to be highly-reliable with low transmission power consumption. In that regard, it is very important to know ranging and position of each device, because that can help to the optimization of the transmission power and to know the position of biological informations obtained from medical implanted device. In this paper, we employ ultra wideband (UWB) systems as the transmission signals, because those achieve the requirements inside human body, high time resolution and low transmission power and to make a smaller device. Thus, we propose a method of position estimation of medical implanted devices inside the human body.

In free space, a type of position estimation algorithm is time-based technique[1]. Such a technique relies on measurements of travel time of signals between nodes. So, range and position can be known because the propagation velocity of microwaves in free space is constant. On the other hand, the human body is formed of various organs with complex structures. Furthermore, each organ has different characteristics of conductivity and relative permittivity. Because, propagation velocity inside human body is expressed as a function of the relative permittivity. For this reason, medical implanted devices placed in different positions cause different propagation velocities due to the EM waves travel through different tissues or organs. Furthermore, the received signal so distorted through the multipath channel caused by the refraction at the boundary of tissues inside human body[4]. As a result, position estimation errors may occur.

In this paper, we suppose the positioning of medical implanted devices in daily life that MRI and CT system don't exist around us. In this condition, a number of anchoring point is set beforehand and we estimate the position of medical implanted devices considering that the medical implanted devices move inside human body like the GPS system. On the premise that diagnostic images of inside human body can be obtained by magnetic resonance imaging (MRI) and computer tomography (CT) at the hospital. In analysis, we use the finite-difference time-domain (FDTD) method[3], which has been widely used to simulate the propagation of electromagnetic waves in biomedical tissues, considering the complex structure of the human body. We analyze the wave propagation inside the human body channel by FDTD method. At first, we calculate the propagation time based on the output of the correlator between the transmitter and the receiver. We apply an adaptive template synthesis method in multipath channel[2] for calculating the propagation time accurately. Furthermore, we estimate the propagation velocity inside human body. We divide the images into regions in order to estimate the relative permittivity of such regions. Then, we estimate the propagation velocity between implanted devices. Finally, we estimate the position of medical implanted devices with a time-based least squares (LS)

positioning approach[4].

This paper is organized as follows: In Section Ⅱ, some basic characteristics of dielectric materials which involve the human body tissue are described. The adaptive template synthesis method in multipath channel is described in Section Ⅲ. The proposed position estimation method is presented in Section Ⅳ. Simulation results are drawn in Section Ⅴ. Finally, conclusions are delineated in Section Ⅵ.

Ⅱ. Radio Propagation in a Medium

A human body consists of various organs with complex structures. Furthermore, each organ has different characteristics of the electrical constants which are conductivity and permittivity.

We should consider the frequency band when we try to estimate the position of implanted devices using UWB radios. Indeed, the electromagnetic wave propagation in dispersive biological tissues is frequency dependent on permittivity and conductivity. The Cole-Cole model[4]. describes the frequency dependency of the complex permittivity. Figure 1 shows the relative permittivity and conductivity of muscle and fat.

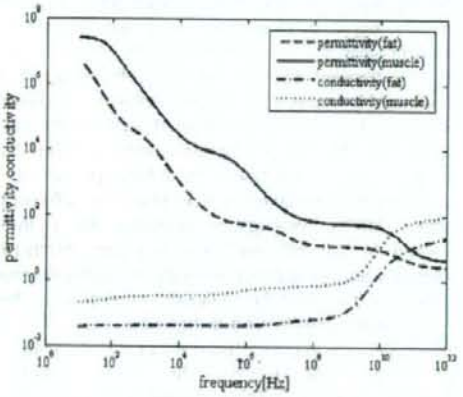

Figure 1- Dielectric parameters of muscle and fat

Furthermore, the propagation velocity of a homogeneous tissue is given by

$$v(\omega) = \frac{c}{\sqrt{\varepsilon_r(\omega)}}, \tag{1}$$

where c is the velocity of light in the free space and $\varepsilon_r(\omega)$ is the relative permittivity of a human tissue. So propagation velocity has frequency dependency and differs by different body tissues. Because of this, a pulse broadening of a received UWB signal is caused by the group delay. Furthermore, the received signal so distorted through the multipath channel caused by the refraction at the boundary of tissues and the channel of frequency dependency inside human body.

Ⅲ. Adaptive Template Synthesis Method

As mentioned above, the received signal so distorted and pulse broadening through the human body channel. When we calculate the propagation time based on the output of the correlator between the transmitter and the receiver in Section Ⅳ, we need to use the template signal considering the received signal distorted and pulse broadening. If we use the template signal not considering the received signal distorted and pulse broadening, estimation errors of the propagation time increase. So we use the adaptive template synthesis method for UWB receiver to calculate the propagation time based on the output of the correlator accurately[2].

The template waveform is constructed as combination of orthogonalized elementary waveforms with certain coefficients. Generally, every UWB signal can be decomposed into some orthgonal elementary waveforms such as sine waves by Fourier series expansion independent of its kernel function. It is therefore possible to approximately construct a UWB template waveform by expanding the UWB signal into the weighted sum of several orthogonal elementary waveforms and truncating it to finite order. The synthesized template waveform is described as

$$w(t) = \sum_{k=1}^{N} C_k \int_{-\frac{T}{2}}^{\frac{T}{2}} L_k(t) \times W_{env}(t) dt, \tag{2}$$

where $L_k(t)$ are the orthogonal elementary waveform and C_k are the Corresponding coefficient. $W_{env}(t)$ is the envelope which truncates each elementary waveform to finite duration. Rectangular window is used as $W_{env}(t)$, that is

$$W_{env}(t) = \begin{cases} 1 \ (|t| \le T/2) \\ 0 \ (others) \end{cases}, \tag{3}$$

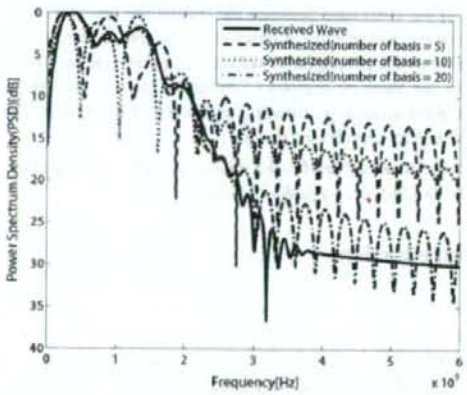

Figure 2- Spectrum of synthesized template waveform and one of the received wave inside human body

Generally, the coefficients C_k are derived as follows

$$C_k = \frac{2}{T} \int_{-\frac{T}{2}}^{\frac{T}{2}} r_s(t) L_k(t) dt, \tag{4}$$

where T is the pulse duration. If the set of orthogonal elementary waveform $L_k(t)$ is complete, the synthesized template strictly matches to the ideal one. In reality, however, the number of coefficient and elementary waveforms should be finite.

In multipath channel such as the human body channel with very close range communication, we mainly consider Intra-pulse Interference (IPI) problem which is occurred when the multipath components are distributed more closely than typical pulse width. We use trigonometric function as orthogonal basis because it is closely-related to frequency domain and there is a possibility that we may analyze the human body channel in frequency domain. Figure 2 shows spectrum of synthesized template waveform and one of the received wave inside human body channel. It can be seen form Figure 2 that synthesized template waveform can well approximate the one of the received wave through the human body channel.

Ⅳ. Proposed Method of Position Estimation

We proposed a position estimation method by estimating the propagation velocity inside of a human body. In addition to it, we calculate the propagation time from arbitrary tag points to node points (whose position is known) by using the estimated propagation velocity. Finally, we estimate the position of medical implanted devices using the LS approach.

The images of inside of the human body are acquired beforehand from a MRI or CT system. Our proposed method uses four medical implanted devices, whose locations are known, and we call them "node" in this paper. On the other hand, there is a medical implanted device, whose location is unknown, and we call it "tag" in this paper.

Our proposed method is composed of two stages. It is very difficult to estimate the real propagation velocity from all arbitrary tag points to node point directly. So, the real propagation velocity is estimated by the images of inside human body obtained from MRI or CT systems beforehand. So, we have large volumes of data of the real propagation velocity. Hence, we estimate the propagation velocity with two stages to simplify the estimation and to reduce the amount of data.

Ⅳ- Ⅰ. First Stage

The procedure of the first stage is as follows. At first, we calculate the average relative permittivity of the region delimited by four nodes. The average relative permittivity ε_{ave} and propagation velocity v_{ave} are calculated as

$$\varepsilon_{ave} = \sum_{i=1}^{I} (\varepsilon_{t(i)} p_{t(i)}), \tag{5}$$

$$v_{ave} = \frac{c}{\sqrt{\varepsilon_{ave}}}, \tag{6}$$

Table 1 - The average relative permittivity of body tissues

Tissue	muscle	fat	blood	intestine
ε_r	47.83	4.08	51.59	50.67
Tissue	lung	stomach	bone	tendon
ε_r	42.56	56.99	17.09	37.61

where i is tissue number, I is total number of tissues, $\varepsilon_{t(i)}$ is the relative permittivity of a homogeneous tissue listed in Table 1[6], and $p_{t(i)}$ is a percentage of the i th tissue.[5]

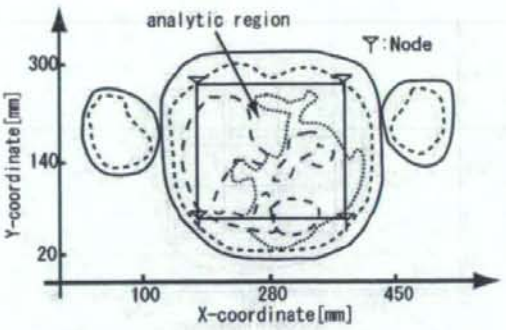

Figure 3- System model of the first stage

Secondly, we calculate the propagation time $t^1_{n(x,y)}$ from four nodes to an arbitrary point in the studied region using v_{ave}. The propagation time in the first stage for the n th node $t^1_{n(x,y)}$ is calculated as

$$t^1_{n(x,y)} = \frac{d_{n(x,y)}}{v_{ave}}, \tag{7}$$

where x is x-coordinate of an arbitrary point, y is y-coordinate of an arbitrary point, $d_{n(x,y)}$ is a direct length of a path from an arbitrary point to the four nodes, respectively. Also, x, y have 1 mm of separation.

Then, we estimate the travel times t_n of the received signal from the tag point to the four nodes by using a correlation receiver. In this approach, the desired estimation is given by the time shift of the template signal that yields the largest cross correlation with the received signal. Finally, we estimate the position of tag using the LS approach.

$$\theta(x,y)_1 = \min \sum_{n=1}^{4} [t_n - t^1_{n(x,y)}]^2, \tag{8}$$

where $\theta(x, y)_1$ is the estimate position of the first stage.

Ⅳ- Ⅱ. Second Stage

In the stage, we use $\theta(x, y)_1$ which is obtained from Equation (8). Firstly, we divide the images inside of the human body into several regions and estimate relative permittivity of a respective region. A relative permittivity of one region is calculated as

$$\varepsilon_j = \sum_{i=1}^{I} (\varepsilon_{t(i)} p^j_{t(i)}), \tag{9}$$

where j is a region number, i is a tissue number, ε_j is an average relative permittivity of j th region, $\varepsilon_{t(i)}$ is the relative permittivity of a homogeneous tissue listed in Table 1, and $p^j_{t(i)}$ is a percentage of the i th tissue in the j th region.

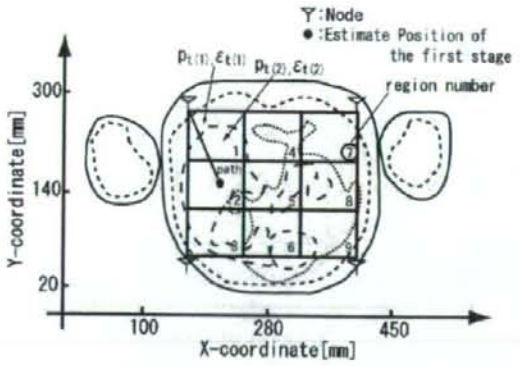

Figure 4- (3×3) regions system model of the second stage

Secondly, we estimate the relative permittivity ε_n and propagation velocity v_n of the paths from four nodes to $\theta(x, y)_1$.

$$\varepsilon_n = \frac{\sum_{k=1}^{K}(\varepsilon_k d_k)}{d_{all}}, \tag{10}$$

$$v_n = \frac{c}{\sqrt{\varepsilon_n}}, \tag{11}$$

where K is a number of regions through the propagation path from the n th node to $\theta(x, y)_1$, d_k is a length of the path through the k th region, and d_{all} is a direct length of the path from n th node to $\theta(x, y)_1$. Then, we calculate the propagation time $t^2_{n(x,y)}$ from four nodes to an arbitrary point using v_n. The propagation time $t^2_{n(x,y)}$ is calculated as

$$t^2_{n(x,y)} = \frac{d_{n(x,y)}}{v_n}, \tag{12}$$

where x is x-coordinate of an arbitrary point, y is y-coordinate of an arbitrary point, and $d_{n(x,y)}$ is a length of a path from an arbitrary point to four nodes, respectively.
And x, y have 1 mm of separation.

Finally, we estimate the position of tag using the LS approach.

$$\theta(x, y)_2 = \min \sum_{n=1}^{4} [t_n - t^2_{n(x,y)}]^2, \tag{13}$$

where t_n is the travel time of the received signal from tag to the four nodes, and $\theta(x, y)_2$ is the estimate position of the second stage.

V. Numerical Simulation

This section presents simulations to demonstrate the performance of the proposed method.

V- I. Simulation Model

The images of MRI or CT system are two-dimensional images. In this paper, we consider only two dimensional images. Figure 5 and Figure 6 show the simulation image obtained by the FDTD of Remcom Co., Ltd. Figure 5 is the image of a cross-section of a human body at high 137.5 cm and Figure 6 is that of a human body at high 157.5 cm. These model contain human body tissues such as muscle, fat, blood, bone, stomach, intestine, bladder, tendon, lung. The following is the characteristic of these models.

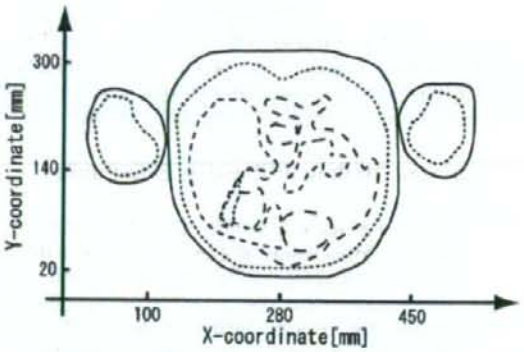

Figure 5- Simplified 2D human body model of 137.5 cm high

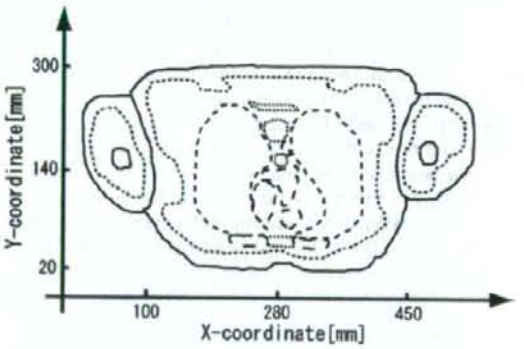

Figure 6- Simplified 2D human body model of 157.5 cm high

As mentioned before, we consider four nodes at positions (171,61), (400,61), (171,240), and (400,240). On the other hand, there is one tag device.

V- II. Performance Evaluation of Proposed Method

We evaluate the performance of our proposed method. In this paper, we consider the human body channel as the static model. At the second stage, we divide the large region inside of the four nodes into some smaller regions. The number of partitions is from (3×3) to (7×7) for x-direction and y-direction. We compare the proposal with the method using the average relative permittivity obtained in Table 1, in order to estimate the propagation velocity from all arbitrary tag points to a node point. The average relative permittivity inside the human body is assumed to be 2/3 of muscle and 1/3 of fat. The proportion of the tissue of high water content (HWC) to the low water content (LWC) is 2:1 in a human body, where the typical tissue of HWC is muscle and fat for LWC. Simula-

tion specifications are listed in Table 2.

Table 2 – Simulation Specification

Analysis Model	Body model of FDTD
Transmit Waveform	Gaussian Mono Pulse
Used Band Frequency	0~4.0 [GHz]
Time Step	1.926 [ps]
Sequence	MLS (length=7)
Pulse Interval	5000 [time step]
Kind of Noise	AWGN

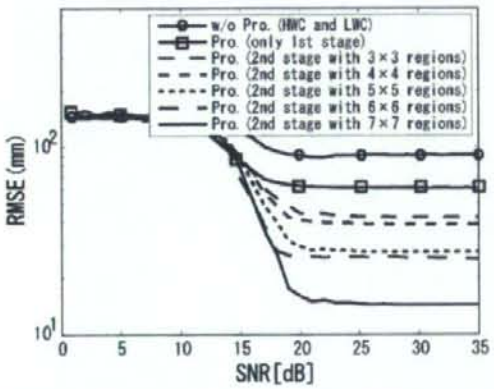

Figure 7- Comparison of positioning error of 137.5 cm high

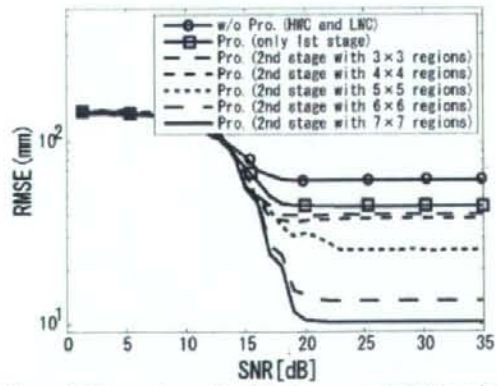

Figure 8- Comparison of positioning error of 157.5 cm high

Figure 7 and 8 show the result of position estimation. The horizontal axis shows SNR and the vertical axis shows RMSE of position estimation. Simulation results show that accuracy of proposed method of positioning is around the size of medical implanted device such as a capsule endoscopes. In addition, simulation results show that when the regions are smaller, the positioning accuracy is better.

VI. Conclusion

In this paper, we analyze the propagation of UWB signals inside of human body tissues with the FDTD method. Especially, we focused on the time-based position estimation of medical implanted devices inside human body. Firstly, we apply an adaptive template synthesis method in multipath channel for calculate the propagation time accurately based on the output of the correlator between the transmitter and the receiver.

Moreover, we have proposed the position estimation method of medical implanted devices using estimation of the propagation velocity inside of the human body. Simulation results show that the proposed method gives a positioning accuracy around the size of medical implanted devices such as capsule endoscopes. In addition, simulation results show that if the regions are smaller, the positioning accuracy is better.

In the future, we estimate the propagation velocity inside human body without prior information of human body images. Furthermore, we expand our 2D model inside human body to 3D model. In 3D model analysis, we additionally need to consider the more complex structure of human body tissues. So the signals refract at the boundary of tissues many times. So we need to estimate so precisely the increase of propagation time based on the refractions of the signal.

References

[1] Sinan Gezici, Zhi Tian, Georgios B. Giannakis, Hisashi Kobayashi, Andreas F. Molisch, H. Vincent Poor, and Zafer Sahinoglu, "Localization via Ultra Wideband Radios," IEEE SIGNAL PROCESSING MAGAGINE, pp70-84, Jul. 2005.

[2] K. Taniguchi and R. Kohno, "Design and Analysis of Synthesized Template Waveform for Receiving UWB Signals," IEICE Trans., Fundamentals, Vol.E88-A, No.9, Sept 2005.

[3] Guilin Sun, Christopher W. Trueman, "Numerical Dispersion and Numerical Loss in Finite-Difference Time-domain Method in Lossy Media," IEEE Trans. Antennas Propag, vol.53 pp3684-3690, Nov 2005.

[4] A. Alomainy, Y. Hao, Y. Yuan, Y. Liu, "Modelling and Characterisation of Radio Propagation from Wireless Implants at Different Frequencies," Proc. The 9th European Conference on Wireless Technology, pp.119-122, Sep 2006.

[5] T. Nakamura, M. Shimizu, H. Kimura, and R. Sato, "Effective Permittivity of Amorphous Mixed Materials," IEICE Trans.B, vol.J87-B No.11, pp.1951-1958, Nov.2004

[6] M. Kawasaki, H. Harada, R. Kohno, "Position Estimation Method of Medical Implanted Devices using Estimation of Propagation Velocity inside Human Body," Proc. ISMICT'07, Oulu, Finland, Dec 2007.

Design of Communication Model Suitable for Implanted Body Area Networks

Shun NAGAMINE, Ryuji KOHNO

Division of Physics, Electrical and Computer Engineering, Yokohama National University
79-5 Tokiwadai, Hodogaya, Yokohama, 240-8501, Japan
Tel: +81-45-339-4116, Fax: +81-45-338-1176
E-mail: shun @kohnolab.dnj.ynu.ac.jp

Abstract

Recently wireless communication has been developed with nano-size devices by semiconductor technology. By means of transmitting vital data, we can observe the body's conditions and detect any possible problem in the human body at anytime. However, not only power consumption of implanted wireless communication devices with a sensor function (node) but also thermal influence on human body should be considered carefully for implementation of such technology. So, it is difficult to apply current sensor network technology directly to the human body. When implanted nodes communicate, it is expected to raise thermal influence caused by the electromagnetic wave exposure and circuit heat. And power-efficient information gathering is preferable that long term continuous duty for implanted nodes if they cannot be recharged. So, we suggest that a sensor network inside the body takes a clustering form and switching leadership between two nodes in order to control their thermal influence. In this paper, we design a communication model. Specifically, we propose network configuration, communication flow, and MAC protocol including alarm mode which is a countermeasure against emergency.

Keywords: Body Area Network, thermal influence, MAC protocol

I. Introduction

With the increased sophistication of semiconductor technology, smaller wireless communication devices have been developed. Nowadays the wireless communication has been developed with nano-size devices by these technologies. In the near future, these advances will make possible to implant wireless communication devices with a sensor function (node) and form a sensor network inside the human body for health monitoring purposes. Such system is generally called implanted body area network (BAN). Each node can monitor health data such as blood pressure, blood glucose level and pulsation, and transmit them to a medical server.

For implementation of such technology, not only power consumption of node but also thermal influence on human body should be considered carefully. So it is difficult to apply current sensor network technology directly to the human body because there is no model considering thermal influence yet. Additionally, when we assume that such technology will be applied to medical systems, it is very important and essential to immediately deal with emergency situation because of being fatal to humans.

A power-efficient information gathering structure is necessary because it is preferable that long term continuous duty for nodes implanted in a human body [1]. In case that implanted nodes cannot be recharged, we anticipate that this demand is higher. The received power depends on the transmission distance, so it is advisable to take a clustering form for controlling power consumption. In a clustering form, neighbor nodes form a cluster, where a full function device (FFD) node is the cluster leader that gathers biometrical data from another node that belong to the cluster. The FFD node interfaces with a medical server outside the body. Therefore, in this paper we adopt the clustering form as a network model. In this case, the leader consumes more power than the other nodes. So, it offers a higher rise of thermal influence caused by circuit heat and electromagnetic wave exposure.

Consequently, we can choose which node is the leader, switch leadership to another node in order to disperse the thermal influence. For temperature rise caused by thermal influence, we employ an approximation of the Pennes' biologic thermal transport equation that is often used as the computation approach of heat propagation in a human body caused by electromagnetic waves and circuit heat.

While communication leader, there are two conditions for it. The leader collects information from all the non-leader nodes (reception mode) and transmits the information to a receiver outside the body (transmission mode). Notice that reception mode takes a longer time since the information of several nodes must be collected. Thus, this longer time increases the risk of thermal influence. So, we proposed a method for controlling the thermal influence by considering MAC [2]. In this paper, we improve the aforementioned protocol.

In Section II, we describe the proposed communication model inside the human body. Specifically, we propose network structure, communication flow, and MAC protocol including alarm mode which is a countermeasure against emergency [3]. Then, We discuss the calculation of temperature

increment and power consumption in Section Ⅲ.We assume that they are evaluation standards. In section Ⅳ, we evaluate the improved MAC protocol by computer simulation and show the effectiveness in point of thermal influence and power consumption. Finally, conclusions are given and we describe future works in Section Ⅴ.

Ⅱ. Design of Implanted BAN Communication Model

A. Network Structure

Since implanted biosensors must operate with very limited power, energy efficiency is an important aspect of design. Prior research shows that a cluster-based communication protocol is more energy efficient than a tree-based approach [4] [5]. Cluster-based communication protocol is based on the idea that energy consumption can be reduced by having particular nodes performing long range communication with a receiver outside the body. These nodes are called cluster leaders. The FFD node is equipped with more complex circuits. So, all the non-leader nodes are denominated as reduced function device (RFD) nodes that contain simple sensors, a processor, and a transceiver. We assume that a cluster consists of a couple of FFD nodes and a number of RFD nodes, see Figure 1.

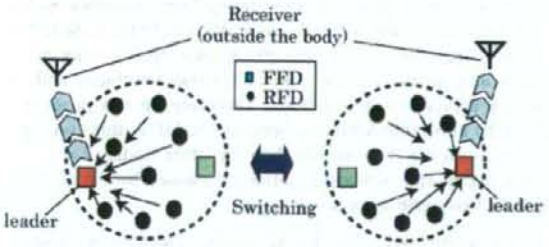

Figure 1- Switching leader structure

We propose switching leadership between a couple of FFD nodes to disperse the thermal influence.

B. Communication flow

We proposed communication flow of the leader and RFD nodes while the leader form a cluster and switch leadership ultimately. Then we describe proposed flowchart in Figure 2.

Initially, the leader allots a unique address for each RFD node to acknowledge the number of them belonging to a cluster. After clustering, the leader broadcasts *backoff data* on the basis of it. Then the leader sleeps for a given period while RFD nodes sense biometrical data. When the leader wakes up, it indicates that and makes each RFD node to stop sensing. After that, the leader gathers biometrical data from all RFD nodes and transmits it to a medical server outside the human body. And then, the leader sleeps again. We define this communication flow as a cycle. The leader switches leadership from itself to another FFD node after a set number of cycles. When the leader switches, each RFD node begin to sleep until a new cluster is formed.

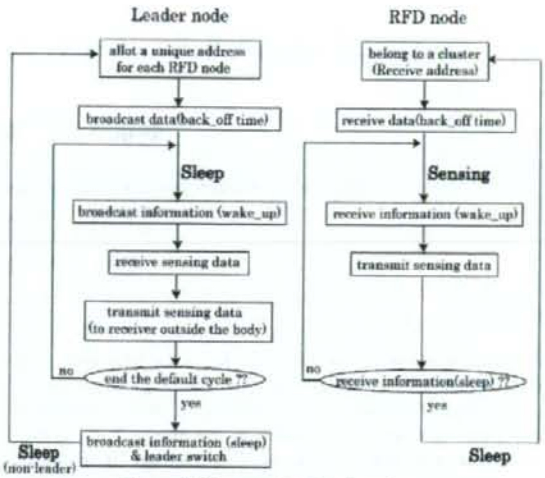

Figure 2-Communication flowchart

C. Proposed MAC protocol

The leader receives the information from a number of RFD nodes in reception mode. So, it is expected that the processing time in that mode changes significantly depending on the number of RFD nodes and media access control. Therefore, we proposed a MAC protocol, which is effective at collecting the information from each node to the leader in order to control the thermal influence. In this paper, we improved our proposed MAC protocol to make communication more efficient.

New proposed protocol adopts carrier sense and backoff, so it is based on CSMA/CA protocol essentially. A term of the carrier senses, that is to say waiting time, is called *backoff time*. A *backoff* is determinant factor of *backoff time*. It is a random integer number that is generated from a uniform distribution in [0, CW]. We propose a new protocol that $CW_{\min}$ is defined as following expression including the number of RFD nodes,

$$CW_{\min} = \alpha M \tag{1}$$

where M is the number of RFD nodes in the cluster, α is the *backoff-coefficient* we defined. This coefficient is chosen from database (Table 1) which is computed preliminarily.

Table 1 - Backoff-coefficient

α	the number of RFD nodes
4.5	~10
4.0	~20
3.5	~30
3.0	~40

RFD nodes transmit sensing data most effectively by choosing appropriate *backoff-coefficient*. Figure 3 shows the simulation result of processing time when the number of RFD nodes is 10.

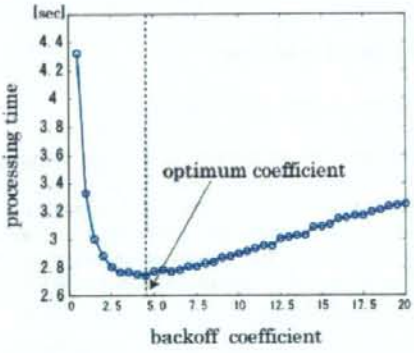

Figure 3- Processing time (10 RFD nodes)

Optimum coefficient of this result is saved as *backoff-coefficient*. Practically, the leader figures out the number of RFD nodes in the cluster and broadcasts *backoff data* whose expression is allotted *backoff-coefficient* depending on the number of RFD nodes like Table 1.

D. *Alarm mode*

Particular demand in medical systems includes a countermeasure against emergency situation. In such cases, it is very important and essential to immediately communicate because of a circumstance to human vitality. So, we need to consider a certain method in an emergency. Then we propose alarm mode which is a function of the proposed MAC protocol .

Alarm mode initiates with transmission of an alarm signal from a RFD node to the leader. When a RFD node detects biometrical data out of healthy range, it transmits an alarm signal to the leader to acknowledge an emergency situation. After receiving the signal, the leader wakes up from sleeping and transmits updated *backoff data* to that node. *Backoff data* is updated as,

$$CW = 1 \quad \text{(constant)}. \tag{2}$$

This algorithm let an alarmed node to transmit biometrical data preferentially each time because that it can transmit with minimal-length waiting consistently. As soon as the leader received all data from that node, it transmits to a medical server outside the human body. Then alarm mode finishes and each node returns to normal mode. We describe a communication flow in alarm mode in Figure 4.

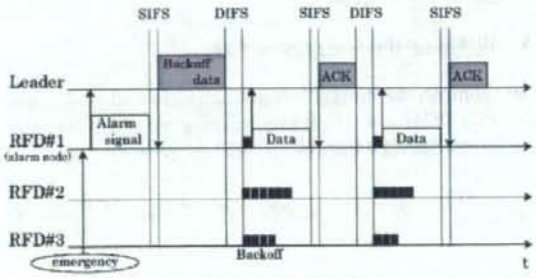

Figure 4- Alarm mode

We compute the time required for the leader to make a medical server know about the emergency to confirm the effectiveness of alarm mode function. In addition, we apply this function to our proposed protocol. So we estimate the simulation result compared with pure ALOHA, CSMA/CA and proposed protocol without alarm mode.

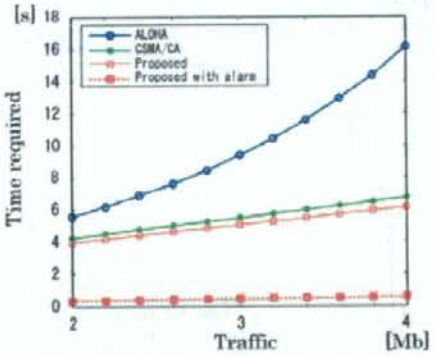

Figure 5- Time required

Figure 5 illustrates the time required depending on traffic. It denotes the characteristic when the amount of biometrical data which RFD nodes sensed changes. This graph shows there is few time required with the alarm mode. We can confirm that updating *backoff data* and reducing *backoff time* enable to receive data from a specific RFD node preferentially.

Additionally, the time required in alarm mode hardly change even if traffic increases. We consider that the increment of traffic affects collision of packets, too. And there is no collision in *alarm mode* because an alarmed node to transmit biometrical data preferentially each time. So it would appear that existence or nonexistence of packet collisions makes a differ-

ence in this result. Consequently, we can evaluate the effectiveness of *alarm mode* function.

Ⅲ. Thermal Influence and Power Consumption

In this section, we explain the thermal influence and power consumption as evaluation standards of our proposed communication model inside the body.

A. Biological thermal propagation

We consider the thermal influence caused by electromagnetic waves (EM) and circuit heat by using the modification of the Pennes' biologic thermal transport equation given by

$$\rho C_p \frac{dT}{dt} = \kappa \nabla^2 T - \rho \rho_b C_b F (T - T_b) + \rho SAR + \frac{V A_{active}}{\rho C}, \quad (3)$$

where ρ is the tissue density, C is the specific heat of the tissue, κ is thermal conductivity of the tissue, T is the temperature of the tissue, F is flow rate of blood, V and A_{active} is the voltage and current of the leader, respectively. The suffix b expresses blood parameter. We calculate the SAR by using the three-dimensional field analytic simulator XFDTD.

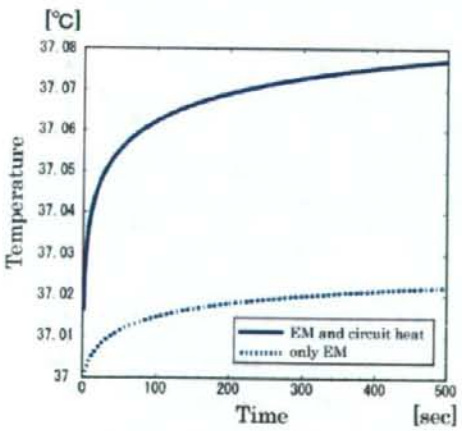

Figure 6- Temperature increment

Figure 6 shows the temporal characteristic of temperature increment when there is no leader rotation. So, the tissue surrounding the leader is heated continuously. In this paper, we assume that the medium in which the leader exists is muscle because it comes in a larger proportion relative to other tissues or organs. Furthermore, muscle is more susceptible to thermal influence than other tissues or organs. From this result, we assume that thermal influence caused by circuit heat is much larger than by electromagnetic waves.

B. Power Consumption

We express the calculation formula of the leader's power consumption divided into communication (active) mode and sleep mode. It is given by

$$\begin{aligned} P_{active} &= T_{receive} \times A_{active} \times V, \\ P_{sleep} &= T_{receive} \times A_{sleep} \times V, \end{aligned} \quad (4)$$

where $T_{receive}$ is the processing time while receiving biometrical data from all RFD nodes. It differs depending on MAC protocols. So the difference of $T_{receive}$ comes to the difference of protocols directly. The value of A and V refers to related study [6].

Ⅳ. Computer Simulation

A. Simulation purpose and setup

We compute the thermal influence and power consumption in proposed protocol compared with the existing protocols ALOHA and CSMA/CA. The purpose of this simulation is to confirm the effectiveness of our communication model in point of these standards. We examine the characteristic when the sleep time of the leader changes. Parameters in this simulation are shown in Table 2.

Table 2 – Simulation setup

parameter	value	parameter	value
bit rate	250kbps	sleep time	1-20sec.
pay load	500bits	Switch cycle	10
slot time	144μs	packet	50
DATA time	2480μs	V	3.0V
SIFS time	192μs	A_{active}	20mA
DIFS time	400μs	A_{sleep}	1μA
ACK time	352μs	the number of RFD nodes	10

B. Simulation result

Figure 7 shows the saturated temperature during a long time, where leaders can switch several times. This result is the characteristic when the sleep time changes in pure ALOHA, CSMA/CA and proposed, respectively.

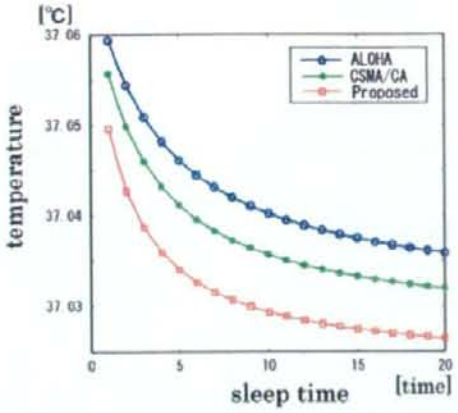

Figure 7- Saturated temperature

Figure 7 shows the saturated temperature during a long time, where leaders can switch several times depending on the sleep time in pure ALOHA, CSMA/CA and proposed, respectively. As shown in Figure 7, it is most affected by thermal influence in ALOHA. We consider the factor of this result is the processing time of receiving biometrical data from all RFD nodes, that is $T_{receive}$. When the value of $T_{receive}$ is large, the switching interval comes to long too. So the time the leader is affected thermal influence by exposing radiation and circuit heat comes to the longest in ALOHA. And then the temperature increment in the proposed protocol is less than ALOHA and CSMA/CA. This result proves that nodes can communicate most efficiently and reduce the thermal influence in our proposed protocol.

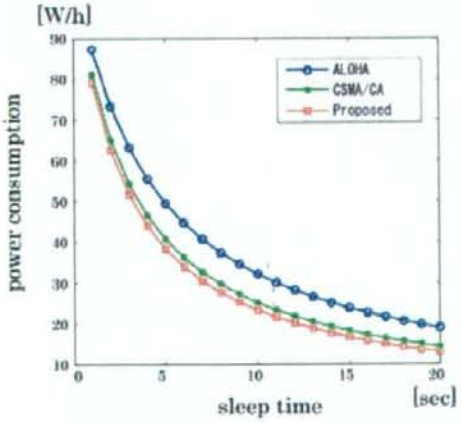

Figure 8- Power consumption

Figure 8 shows the power consumption of the leader in an hour. The proposed protocol can control power consumption better than ALOHA and CAMS/CA because the processing time of receiving data is the factor that influences power consumption directly, too. However, there seems to be less difference between the proposed protocol and CSMA/CA compared to the result of Figure 7. We consider that while differences of power consumption depends mostly on differences of the processing time, differences of thermal influence depends on differences of circuit heat and exposing radiation time caused by increase of the processing time.

V. Conclusion

In this paper, we design a communication model such as network structure, communication flow and MAC protocol in an implanted body area network. We also show the effectiveness of our communication model in terms of thermal influence and power consumption.

In a future work, we plan to consider optimum sleep time on the basis of update rate which has relationship of tradeoff with sleep time. Moreover, we will propose the metrics which evaluates comprehensively and compare with the existing protocol.

References

[1] W. R. Heinzelman, A. Chandrakasan, and H. Balakrishnan, "Energy-Efficient Communication Protocols for Wireless Microsensor Networks "In Hawaii International Conference on System Sciences, 2000.

[2] Shun Nagamine, Hiroki Harada, Ryuji Kohno, "Novel MAC Protocols Considering Thermal Influence in an Implanted Body Area Network" Second International Symposium on Medical Information & Communication Technology on 11-13 Dec. 2007.

[3] O. C. Omeni, O. Eljamaly, A. J. Burdett, "Energy Efficient Medium Access Protocol for Wireless Medial Body Area Sensor Networks" Medical Devices and Biosensors, 2007. ISSS-MDBS 2007. 4th IEEE/EMBS International Summer School and Symposium on 19-22 Aug. 2007.

[4] Shankar, V. Natarajan, A. Gupta, S.K.S. Schwiebert, L. Dept. of Comput. Sci. Eng., Arizona State Univ., Tempe, AZ, USA, "Energy-efficient protocols for wireless communication in biosensor networks" Personal, Indoor and Mobile Radio Communications, 2001 12th IEEE International Symposium on 30 Sept.-3 Oct. 2001.

[5] Qinghui Tang, Naveen Tummala, Sandeep K. S. Gupta, Senior Member, IEEE, and Loren Schwiebert Senior Member, IEEE, "Communication Scheduling to Minimize Thermal Effects of Implanted Biosensor Networks in Homogeneous Tissue" Biomedical Engineering, IEEE Transactions on July 2005.

[6] Timmons, N.F. Scanlon, W.G., "Analysis of the performance of IEEE 802.15.4 for medical sensor body area networking", Sensor and Ad Hoc Communications and Networks, 2004. IEEE SECON 2004. 2004 First Annual IEEE Communications Society Conference on 4-7 Oct. 2004.

Performance Analysis of Pulsed Chirp UWB Schemes used Hopping Sequence for Wearable Wireless Body Area Network

Hideki Mochizuki[a], Makoto Kawasaki[a], Shun Nagamine[a], Igor Dotlic[b], Ryuji Kohno[a,b]

[a] *Division of Electrical and Computer Engineering, Faculty of Engineering, Yokohama National University, 79-5 Tokiwadai, Hodogaya, Yokohama, Kanagawa, 240-851, Japan*

[b] *Medical ICT Institute, National Institute for Information and Communication Technology, 3-4 Hikarino-oka, Yokosuka, Kanagawa, 239-0847, Japan*

Abstract

In this paper, we compare conventional coherent low data rate IR UWB (DS-UWB, Chirp on UWB) and our proposed system of pulsed chirp UWB with or without frequency hopping. IEEE 802.15.4a channel model has been utilized for BER evaluation under multi pico-net interference conditions. Our results show that proposed pulsed chirp UWB with frequency hopping has superior performance compared to conventional methods.

Keywords: ***Body Area Network, Ultra Wide Band, Frequency Hopping***

1 Introduction

Recently, there has been considerable amount of research effort directed towards applied information and communications technology to medical services [1, 2]. As main concept, WBAN (Wireless Body Area Network) has been researched. WBAN are networks composed of wireless communication inside, outside or between inside and outside of the human body. Communication between devices located outside of a human body is called Wearable WBAN; similarly, wireless network composed of devices located inside of a human body is called Implanted BAN.

In this work, we will limit our discussion to Wearable WBAN. Wearable WBAN is expected to have numerous applications. For example, sensors can continuously measure and transmit vital parameters data via wearable WBAN.

Since Wearable WBAN is consistent of small, autonomous network nodes, the consequent low transmission power is required for their longer battery life. Vital signs are important information, so it is important to achieve privacy. Furthermore, medical information and communication technology has need for data rates of about 10 kbps. Considering practical purposes, however, it is necessary to achieve higher data rates.

On the other hand, a lot of attention has been paid to UWB (ultra wideband) wireless communications systems due to their great potential to reach high data rates in wireless communications. UWB signal is defined as one with relative bandwidth (bandwidth/center frequency) surpasses either 20% (for consumer use) or 25% (for military use). In addition to the possible implementation of high speed wireless access with over 1 Gbps data-rates, UWB systems also have the potential to simplify the RF circuitry of the transceivers and lower the transmit power. These features correspond with the demand for the wearable WBAN communications.

In this paper, we compare conventional low data rate IR UWB (DS-UWB, Chirp on UWB) and our proposed system of pulsed chirp UWB with or without frequency hopping. IEEE 802.15.4a channel model has been utilized for BER evaluation under multi pico-net interference conditions.

2 UWB communication technology

2.1 DS-UWB system

2.1.1 Transmitter's Description

The transmitted signal for DS-UWB using the spreading sequence of the sequence length N, denoted $f(t)$, is given by

$$f(t) = \sum_{j=0}^{N-1} m_j \delta(t - jT_c) . \qquad (1)$$

Here, $\delta(t)$ represents the transmitted monocycle waveform, m_j is the j-th component of the spreading sequence and T_c is the chip width. We assume that $f(t)$ consists of N pulses.

2.12 Receiver's Description

The received signal $f_{rec}(t)$ is represented by

$$f_{rec}(t) = \sum_{j=0}^{N-1} m_j \delta(t - jT_c) + n(t) , \qquad (2)$$

Where $n(t)$ represents additive white Gaussian noise (AWGN) and multiuser interference (MUI). At the receiver, the spreading sequence is assumed to be known and the template function to be correlated with the received signal is assumed to be the same as the transmitted signal. Thus the signal generated at the receiver, $f_{rep}(t)$ is given by

$$f_{rep}(t) = \sum_{j=0}^{N-1} m_j \delta(t - jT_c). \quad (3)$$

The correlation function $R(\tau)$ between $f_{rec}(t)$ and $f_{rep}(t)$ is calculated as

$$R(\tau) = \int_{-\infty}^{+\infty} f_{rec}(t) f_{rep}(t-\tau) dt. \quad (4)$$

Transmitted symbol is decided by calculating $R(\tau)$.

2.2 Chirp on UWB system

2.2.1 Characteristics of chirp on UWB

The chirp waveform is represented by

$$s(t) = \begin{cases} \cos(\theta(t))(0 \le t \le T) \\ 0(otherwise) \end{cases}. \quad (5)$$

$\theta(t)$ is the change of phase depending on time. In the case of liner chirp, chirping rate $\mu(t)$ is constant so that frequency $f_M(t)$ is liner function with the respect to t and $\theta(t)$ is a quadratic function.

$$f_M(t) = f_0 + \mu(t), \quad (6)$$

$$s(t) = \cos(2\pi f_0 t + \pi \mu t^2). \quad (7)$$

Band width B is a function of time duration T and chirping rate μ.

$$B = |\mu| T. \quad (8)$$

Chirp on UWB waveform is made by multiplying root raised cosine pulse and linear chirp. Root raised cosine pulse $r(t)$ is represented by

$$r(t) = \frac{4\beta}{\pi\sqrt{T_p}} \frac{\cos\left[\frac{(1+\beta)\pi t}{T_p}\right] + \frac{\sin\left[\frac{(1-\beta)\pi t}{T_p}\right]}{\frac{4\beta t}{T_p}}}{(\frac{4\beta t}{T_p})^2 - 1}. \quad (9)$$

$\beta=0.6$ is roll-off factor. Using this pulse, Chirp on UWB waveform is represented by

$$P_{cou}(t) = \begin{cases} r(t)\exp(-j\frac{\pi\alpha t^2}{2})(-\frac{T}{2} \le t \le \frac{T}{2}) \\ 0(otherwise) \end{cases}. \quad (10)$$

2.2.2 Chirp on UWB system model

In this section, we describe Chirp on UWB system. Data $b(t)$ was modulated by chirp waveform $P_{cou}(t)$. Transmitted waveform $s(t)$ is represented by

$$s(t) = b(t) P_{cou}(t). \quad (11)$$

Each user is assigned a frequency band of *500 MHz* and positive or negative chirp slope, as defined in table. 1. Description of the Chirp on UWB receiver is the same as DS-UWB one.

3 Pulsed Chirp UWB method

In this section, we describe two proposed Pulsed Chirp UWB methods. Proposed method 1 does not use frequency hopping. Proposed method 2 uses frequency hopping between used bands.

In this paper, we used Reed-Solomon (RS) sequence and One Coincidence Code (OCC) sequence as a frequency hopping sequences. Thereinafter we will show details of proposed methods.

Table 1: User assigned bands and chirping slopes.

user	Chirping rate	Center frequency f_c[GHz]
1	$\mu \square 0$	3.25
2	$\mu \square 0$	3.25
3	$\mu \square 0$	3.75
4	$\mu \square 0$	3.75
5	$\mu \square 0$	4.25
6	$\mu \square 0$	4.25
7	$\mu \square 0$	4.75
8	$\mu \square 0$	4.75

3.1 Proposed method 1

Transmitted waveform $f(t)$ is

$$f(t) = \sum_{j=0}^{N_s-1} m_{i,j}(s_{i,j}(t - jT_f)) \quad (12)$$

$$(c_{i,j} = 1 \rightarrow m_{i,j} = 1, c_{i,j} = 0 \rightarrow m_{i,j} = -1)$$

T_f is time frame, $c_{i,j}$ is j-th element of PN sequence assigned to the i-th user; N_s is the length of the PN sequence. Similarly, $s_{i,j}$ is a waveform of the j-th corresponding pulse for the i-th user. Chirp pulse waveforms $s_{i,j}$ are described in detail below.

First, maximum and minimum value of used frequency is defined - f_{max} and f_{min} respectively. Second, we divide the bandwidth by applied length of sequence. Bandwidth B and chirped bandwidth Δf are

$$B = f_{\max} - f_{\min}, \quad (13)$$

$$\Delta f = \frac{B}{N}. \quad (14)$$

All central frequencies of used frequency bands are defined as $f_{c1}, f_{c2}, \ldots f_{cNs}$. Frequency hopping sequence of the i-th user is defined as

$$f_i = (f_{ci}, f_{c(i+1)} \cdots f_{c(i+N_s-1)})$$
$$(f_{ci} = f_{c(i+N_s)} = \ldots = f_{c(i+nN_s)} = \ldots) \quad (15)$$

Chirping rate of j-th chip of i-th user is calculated as

$$\mu_{i,j} = \frac{\Delta f}{T} m_{i,j}, \quad (16)$$

(17)

Here, τ denotes pulse width. Fig. 1 illustrates described principle.

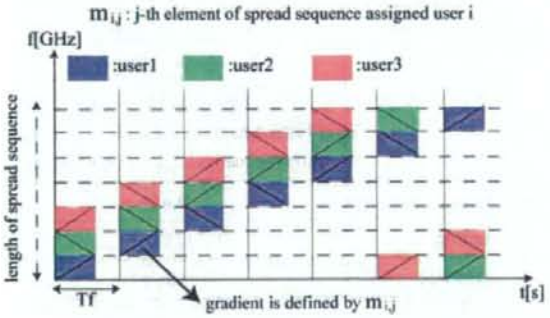

Figure 1: Frequency hopping of proposed method 1.

Finally, chirp pulse waveform of the *j*-th chip for the i-th user, $s_{i,j}(t)$, is represented as

$$s_{i,j}(t) = \begin{cases} r(t-\frac{T}{2})\exp(-j\omega_{i,j}(t))(0 \le t \le T) \\ 0(otherwise) \end{cases}, \quad (18)$$

$$\omega_{i,j}(t) = 2\pi f_{i,j}(t-\frac{T}{2}) + (\frac{\pi\mu_{i,j}}{2})(t-\frac{T}{2})^2. \quad (19)$$

For this method, f_{c1}~f_{cN_s} are defined in table. 2.

Table 2:Frequency divided each center frequency (length of sequence 7)

	Center frequency f_c[GHz]		Center frequency f_c[GHz]
1	3.228	5	4.257
2	3.485	6	4.514
3	3.742	7	4.771
4	3.999		

3.2 Proposed method 2

In this section, we will describe proposed method 2 which uses RS sequence or OCC sequence to determine occupied frequency band. Transmitted waveform $f(t)$ remains the same as in the method 1 (12). Maximum value of applied frequency is defined f_{max}, and minimum is defined f_{min}, so bandwidth B and chirped band width Δf are also as before (13),(14). In this paper, length of RS sequence is 8, and length of OCC sequence is 10. In contrast with method 1, here, bandwidth B is divided in somewhat smaller frequency bands, denoted as $f_1 f_2 \ldots$. Center frequency of each frequency band is denoted as $f_{c1} f_{c2} \ldots$. Defining n_i as hopping sequence of user i, f_{useri} which is applied frequency of user i is represented by

$$f_{useri} = (f_{n_i(1)}, f_{n_i(2)}, \ldots, f_{n_i(j)}, \ldots). \quad (20)$$

Chirping rate is represented by

(21)

(22)

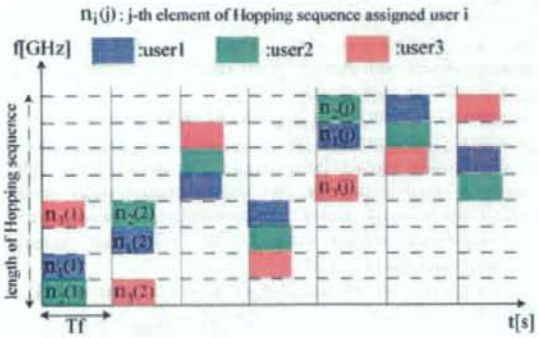

Figure 2: Frequency hopping of proposed method 2.

Fig. 2 illustrates described principle.

Accordingly, chirp pulse waveform for *j*-th chip of *i*-th user $s_{i,j}(t)$ is represented by

$$s_{i,j}(t) = \begin{cases} r(t-\frac{T}{2})\exp(-j\omega_{i,j}(t))(0 \le t \le T) \\ 0(otherwise) \end{cases}, \quad (23)$$

$$\omega_{i,j}(t) = 2\pi f_{cn_i(j)}(t-\frac{T}{2}) + (\frac{\pi\mu}{2})(t-\frac{T}{2})^2. \quad (24)$$

This time, f_{c1}~f_{cN_s} are defined in table.3, for both RS and OCC frequency hopping sequences.

4 Wearable WBAN

Wearable WBAN is different from usual indoor and outdoor UWB propagation models. Propagation through the body is negligible in the gigahertz frequency range and can be ignored. In the Wearable WBAN, path loss is defined for the distance traveled by the wave around the perimeter of the body, not a shortest path distance between transmitter and receiver.

Table 3: Frequency divided each center frequency
(length of RS sequence 8 and OCC sequence 10).

	Center frequency f_c[GHz]			Center frequency f_c[GHz]	
	RS	OCC		RS	OCC
1	3.2125	3.19	6	4.3375	4.09
2	3.4375	3.37	7	4.5625	4.27
3	3.6625	3.55	8	4.7875	4.45
4	3.8875	3.73	9		4.63
5	4.1125	3.91	10		4.79

Furthermore, in the IEEE 802.15.4a Wearable WBAN channel model there are two clear clusters of multi-path components. The first cluster is due to diffraction of the wave around the torso. The second cluster is due to a reflection from the

ground; hence, it strength depends on the electrical properties of the floor material.

We assume that multi-nodes which are taken on body are synchronized. In this paper, we consider that effect of interference wave which is asynchronous transmitted (multi pico-net interference). We assume IEEE 802.15.4a BAN channel model with AWGN. Two scenarios of multi pico-net interference are considered.

Scenario 1 is assumes equal power of all interferers.

Scenario 2 assumes that SIR is defined as average power of all interference signals. For example, if declared SIR is –5dB, number of interference user is 3 and distribution range of SIR is ±5dB, interference wave 1 can be –7dB, interference wave 2 –3dB and interference wave 3 –5dB. Therefore, average interference power is –5dB.

In this paper, we assume that distribution range of SIR is –5dB. Fig.3 illustrates example of interference scenario 2.

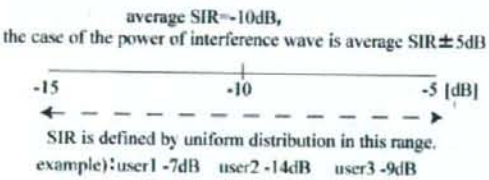

Figure 3: example of interference scenario 2.

5 Simulation

5.1 Simulation setup

Simulation setup is shown in table 4 and table 5. Transmitted pulse waveform is root raised cosine pulse with roll-off factor equal to 0.6. In this simulation, we consider multi pico-net interference. At the receiver, the spreading sequence is assumed to be known and it is perfectly synchronized.

Table 4: Simulation setup of conventional method.

Transmit signal	DS-UWB Chirp on UWB (CoU)
Spread Sequence	DS-UWB: Gold sequence (length:7)
Frequency band	3-5GHz (τ=0.75ns)(DS-UWB) (τ=3ns)(CoU)
Sampling Time	0.3125[ns]
Bit rate	10Mbps
Transmitter position	Front body
Receiver position	Arm
Number of interference pico-net	8
Ground	Concrete

5.2 Simulation results

The BER (Bit Error Rate) characteristics under multi pico-net interference are shown in Fig. 4 and Fig. 5. Fig. 4 shows BER characteristics in the case of 8 pico-net and interference scenario 1. Fig 5 shows BER characteristics in the case of 8 pico-net and interference scenario 2. When SIR is low, Chirp on UWB is superior to others. This is because Chirp on UWB is resistant to near-far problem.

Table 5: Simulation setup of proposed method.

Transmit signal	Pulsed chirp UWB
Spread Sequence	Gold sequence (length:7)
Hopping sequence	RS sequence (length:8) OCC sequence (length:10)
Pulse width	Propose method 1: 2.5[ns] Propose method 2 with RS: 2.5[ns] Propose method 2 with OCC: 3[ns]
Frequency band	3-5GHz
Sampling Time	0.3125[ns]
Bit rate	10Mbps

When SIR is high, proposed method is superior to conventional methods. This is because proposed method is combined characteristic of Chirp on UWB and DS-UWB. Furthermore, proposed method 2 which uses hopping sequence is superior to proposed method 1.

This is because, in the case of proposed method 2, probability of collision on the same frequency band is lower than in the case of proposed method 1.

Comparing method 2 with RS and OCC sequence; length of the OCC sequence is adjusted to length of gold sequence. In this case, the proposed method 2 with OCC sequence is similar to the proposed method 2 with RS sequence. If length of sequence is long, however, the difference of lengths will affect BER characteristics.

From the Fig. 5, we can see that proposed method is superior to conventional methods in the case of interference scenario 2, with interference waves come with various power.

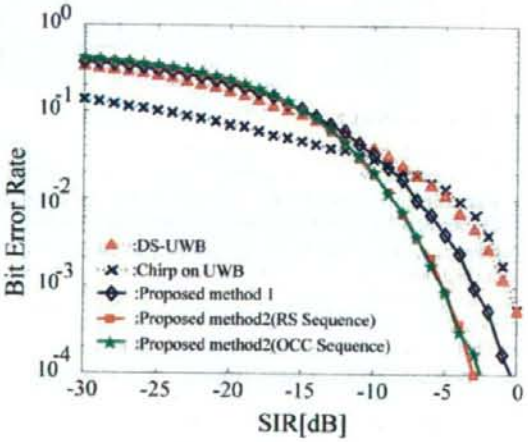

Figure 4: BER characteristics of 8 pico-net.

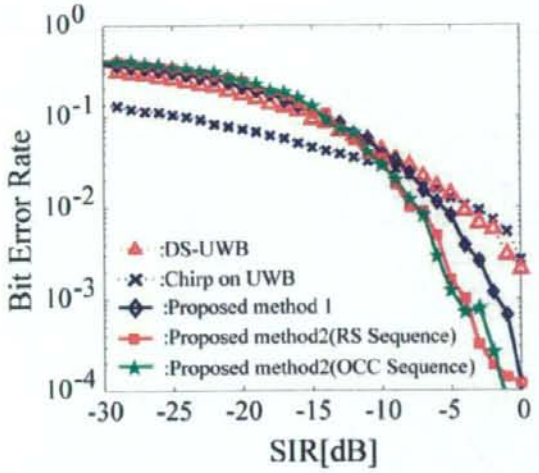

Figure 5: BER characteristics of 8 pico-net, distribution range of SIR is ±5dB.

6 Conclusions

In this paper, we compared conventional methods of UWB IR with proposed method of pulsed chirp with and without frequency hopping. Proposed method with hopping sequence and proposed method without hopping sequence were tested on the scenario of multi pico-net interference.

Both proposed methods with and without hopping sequence are superior to conventional methods. Especially in the case of scenario 2, which assumes interference received with various powers, proposed method is superior to conventional methods.

For a future research, we will consider interference to and from narrowband system. Also, we will propose a system model suitable for Implant WBAN.

References

[1] Andrew Fort, Julien Ryckaert, Claude Desset, Philippe De Doncker, Piet Wambacq, Leo Van Biesen. Ultra-Wideband Channel Model for Communication Around the Human Body. *0733-8716,2006 IEEE*

[2] Daniele Domenicali, Maria-Gabriella Di Benedetto. Performance Analysis for a Body Area Network composed of IEEE 802.15.4 devices. *1-4244-0871-7/07,2007 IEEE*

[3] Andresa F.Molisch Balakrishnan, Dajana Cassiloli, Chia-Chin Chong, Shahriar Emami, Andrew Fort, Johan Karedal, Juergen Kunisch, Hans Schantz, Ulrich Schuster, Kai Siwiak. IEEE802.15.4a channel model-final report.

[4] LAN/MAN Standards Committee of the IEEE Computer Society. Wireless Medium Access Control (MAC) and Physical Layer (PHY) Specifications for Low-Rate Wireless Personal Area Networks. *Draft P802.15.4a/D1.December, 2005(Amendment of IEEE Std 802.15.4-2003)*

Routing Algorithm to Decrease Transmission Delay and Traffic Quantity using Priority Area in Sensor Network of Hospital

Koji Enda, Ryuji Kohno

Yokohama National University
79-5 Tokiwadai, Hodogaya-ku, Yokohama, Kanagawa, Japan

Abstract

Recently, demand of high-speed and high reliability wireless communication in hospital increases. In this paper, we propose the routing algorithm to communicate effectively using position estimation by each sensor or node. ***This propagation channel is modeled to by path loss or Non-line-of sight (NLOS).*** *Geometric efficiency for communication is computed by position of destination node, transmission node and relay node, which are in the range of transmission (of each other). Moreover, Back-off time of carrier sense multiple access with collision avoidance (CSMA/CA) is computed under the influence of this efficiency. Then, by canceling communication for one relay node in the case of detecting transmission of (the) other relay nodes, traffic quantity can decrease. Furthermore, the arrival rate of emergency packet can be improved by adjusting the cancel process of communication for relay node.*

Keyword:

Ad-hoc network, Routing, Network in hospital, Position information

1. Introduction

Medical institutions or hospitals require medical networks for connecting among the medical devices. (In addition, higher reliability and higher throughput are desirable for the medical networks.) Medical network is focused on wireless network (with low cost implementation). One of the most attractive candidates for the low cost (implementation) is ad-hoc network. Ad-hoc network has inherent features, such as the absence of infrastructure, tolerance of link disconnection and flexibility of network topology. In the research of ad-hoc network, many routing algorithm studies as well as studies on positioning algorithm are discussed. Especially, we have introduced positioning system of sensor device for medical institute in ISMICT 2007. Therefore, we focus on routing algorithm that utilizes position information. This position information enables to improve communication efficiency or reliability in routing process. Here, there are several conventional routing algorithms being studied. Most basic routing algorithm is Flooding method. Roughly speaking, in flooding, when one node receives a data packet, the node (simply) retransmits the same packet. This algorithm can fulfill high packet arrival rate because all nodes in transmission range relay individually. However, this method increases traffic quantity of data packet excessively by the individual transmission of all nodes. As the next conventional routing algorithm, there is the Table driven algorithm which configures route utilizing link information with near node. This algorithm can diminish the traffic quantity of data packet, however, the traffic quantity of beacon increases because link table need to be kept newest information of network constantly. Furthermore, this algorithm has the problem of link disconnection by node's movement or reception power insufficiency in real situation. In order to avoid it, it is effective to communicate using strong connection node. However, system of such a method needs to communicate with short distance node inevitably. Therefore, hopping number increases and geometric efficiency is degraded. In other word, if high-reliability communication is desirable in table driven algorithm, packet arrival delay and traffic quantity increases necessarily compared with normal Table driven algorithm. As a last conventional method routing algorithm, there is packet relay control scheme based on priority region (PRCSPR) which is based on aforementioned Flooding algorithm and utilize position information. This method is that if one node detects other node's transmission of same packet, the detected node cancels its transmission. Additionally, according as distance between transmission node and reception node, the reception node is assigned priority of transmission. This enables to restrain traffic quantity in network. In this paper, we solve the problem of increase traffic quantity in Flooding method and link disconnection in Table driven method. Furthermore, we propose effective multi-hop routing method using the position information of each node. This method is based on PRCSPR and CSMA/CA as MAC protocol. This detailed method is described as follows. Firstly, one node senses other node's signal. Next, if it senses transmission finish of others, it waits back-off time and its transmission is started. If the packet same as reserved packet in one node is transmitted from other node, one node cancels its transmission in aforementioned at PRCSPR. In addition, back-off time is decided according as distance between transmission node position and reception node position. In other word, we model back-off time decision function (BOTDF) so as to communicate with multi-hop using the node which exists in geographically effective position. As the demerit of this method, packet arrival rate is degraded comparing with Flooding method. In general situation, if the route from transmission start node to the destination node cannot be configured, same data packet need to be transmitted again at other route. This causes the degradation of throughput and reliability.

Especially for the network in hospital, we must consider the emergency packet, for example, deterioration of patient's condition. In order to enhance the arrival rate of this emergency packet, we propose the postponement method of packet transmission cancel of PRCSPR. This method is able to improve packet arrival rate because possibility of a route disconnection could be suppressed by postponing node's transmission and compensating the route by using other route in case of link disconnection. In other word, one node does not cancel on sensing FIRST transmission of the other node but it cancels instead upon sensing the SECOND transmission of the other node. This process becomes redundant algorithm and enables to improve reliability of emergency packet's communication by restoring disconnected route.

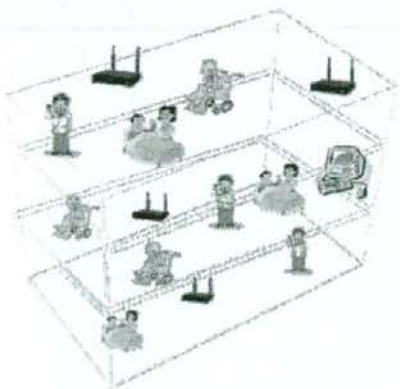

Figure 1. Network in Hospital

2. System Model and Routing Algorithm

2.1. System Model

The devices for communication consist of mobile nodes and anchored nodes. Mobile nodes estimate their own position information through communication with anchored node that has knowledge of its own position. Furthermore, it is assumed that all nodes know other nodes' positions mutually. Each node transmits signal at the same power constantly and therefore the max transmission range have to be constant. Some combinations of each node are under influence of non-line-of sight (NLOS). Therefore, this causes attenuation of received signal strength, shortening of max transmission range and link disconnection. In this paper, we configure the packet link propagation model for communication with neighbor node as the (model integrating these factors).

2.2. Simplified Propagation Model

Mentioned in section 2.1, there is the link disconnection of each node by several elements in real situation. In order to simplify it, we introduce the packet link propagation function (PLPF). PLPF is the function which shows whether nodes are connectable or not by distance between transmission node and reception node. Generally, link connectivity is decreased at long distance (near maximum transmission range). Furthermore, the longer the distance, the larger NLOS probability is. Therefore, we adopt exponential function as the probability distribution function of link connectivity representing these factors. This is shown in equation 1.

$$P_{link} = 1 - \exp(\frac{x-\alpha}{C_p}) \quad (1)$$

Where α is the maximum transmission range, x is the distance between transmission and reception node and Cp is a constant that represents propagation features. This equation is shown in figure 2.

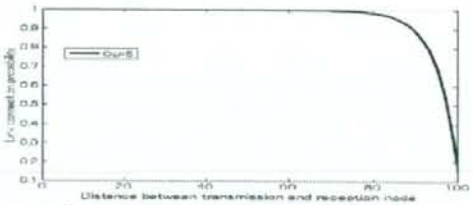

Figure 2. Connection Probability Function by Distance Between Nodes

2.3. Carrier sense multiple access with collision avoidance

This media access control (MAC) protocol is the method for multi-user coexistence communication. Firstly, one node checks the transmission of other nodes. If one node senses transmission of other nodes, it waits until the current transmission of other node to finish before attempting to start its own transmission. Additionally, it waits for a back-off time which is randomly defined by the system. Finally, one node transmits own packet after the back-off time.

2.4. Routing Algorithm

2.4.1. Flooding Algorithm

This routing algorithm is the basic algorithm in ad-hoc network. If one node receives data packet, it transmits the same packet around node. If one node receives the same packet from other nodes, it discards the packet and do not retransmit it again. Thus, this method allows the packet to arrive at the destination node by iteration of these processes. Since flooding method is the algorithm communicated by all possible nodes, the merit is that high packet arrival rate can be fulfilled. However, there is the problem where network traffic quantity increases, radio-wave utilization efficiency decreases and this would lengthen the packet arrival delay. This also causes degradation of throughput.

2.4.2. Table Driven Algorithm

This method is that one node transmits beacon to neighbor nodes and creates a table of connection of each other. The route from transmission node to destination node is created in the table. The merit of this method is it requires only minimal process of transmission in relation to data communication. However, since the link table of each node needs to be kept updated constantly, it is necessary for node to transmit beacon to each other at frequent intervals. Furthermore, this method has the problem of link disconnection. This link disconnection is caused, for example by non-line-of sight or by insufficiency of signal power. Relating to the insufficiency of power, in spite that one node estimates the link connectivity from the received beacon, there is the case that the required power for valid communication cannot be fulfilled and packet also cannot

arrive at the node. In the case where it is impossible to configure a particular route to the destination node, it is necessary to reconfigure to another route and retransmit. The more these retransmission processes occur, the more the throughput decreases. In order to avoid it, it would be effective to adopt a multi-hop way of using the neighbor node that exists within short distance and has strong link connection power. However, such a method is ineffective geometrically because number of packet transmission increases.

2.4.3. Packet Relay Control Scheme Based on Priority Regions

This method is based on the Flooding method. Procedure of this algorithm works as follows. Firstly, a node estimates the distance between transmission node and reception node by position information from GPS or received signal strength. Secondly, priority of packet transmission is decided according to the distance estimated. The longer the estimated distance between nodes becomes, the shorter the back-off time of CSMA/CA becomes and the higher the priority of packet transmission is. This node reserves the packet transmitted from other nodes before forwarding it and waits for a certain back-off time. If one node senses the same packet from other nodes' transmission, this node would cancel its own packet transmission. This reduces the traffic quantity compared to Flooding method. The problem is the rate of link disconnection increases with this transmission cancellation process.

3. Proposed Method

In this section, we state our proposed method. This method is based on PRCSPR in sect 2.2.3. Firstly, relay node (named A) receives packet from transmission node (named B) which contains the position information of B and destination node (named C). The priority of transmission of each node in the selected route is determined by combination of A, B, and C position. Using this position information, priority of each relay node is decided by geographical efficiency of node distribution. To effectively apply the priority values, the back-off time of CSMA/CA for each node in route is determined according to the priority value. The way of geographical efficiency decision is explained as follows. First, the distance between A and B is configured as X_D. Taking the direction angle of node B to C as the reference angle $\theta=0$, the angle from B to A is configured as θ. B's position is configured as the center of circle with maximum transmission range, α as radius of this circle. Additionally, the projected distance of distance node B to relay node A on the transmission direction line towards destination node C is configured as Xs. This Xs represents the geometric efficiency toward C. These are shown in figure 3.

By the way, we consider the "random" distribution of relay node within the circle to be applied to the adaptation of back-off time of CSMA/CA at each node. Therefore, it is ideal that back-off time is allocated uniformly.

PRCSPR method uses nodes within the maximum transmission range. However, the necessary area to arrive at destination node for packet is only half of the disk area of destination node side. Therefore, by limiting number of relay node and back-off time distribution within the half-disk area, delay caused by back-off time can be decreased effectively. Next, in order to apply this uniform allocation of back-off time in the case of half-disk area, we create back-off time decision function such that back-off time is allocated uniformly versus Xs (distance to direction at destination node).

Xs represents geometrical efficiency toward destination node. Xs is shown in equation 2.

$$Xs=X_D\cos\theta \qquad (2)$$

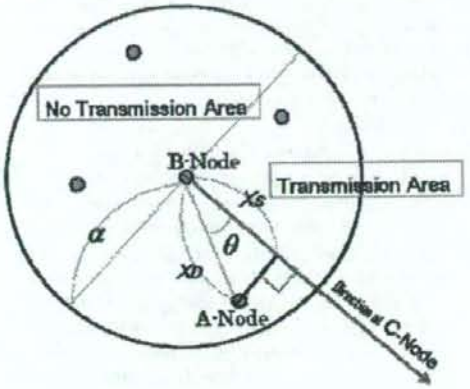

Figure 3. Processing Position Information

Here, it is necessary to calculate geometric area. In aforementioned, half-disk area covering the direction line to destination node C is illustrated. First, the chord line that intersects orthogonal to the Xs is drawn. The shaded area between the chord and the curve of the circle is calculated as As. Then, the ratio of the shaded area to the half-disk area, A is defined as back-off time decision function. "Former area away vertical line of Xs" is illustrated in figure 4.

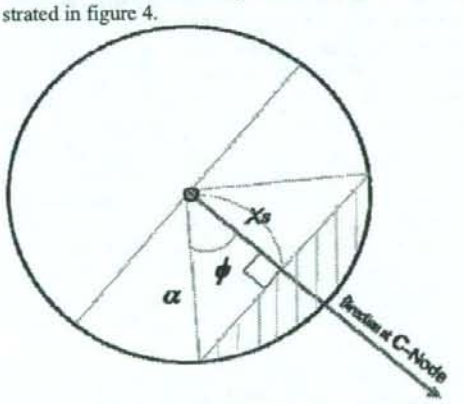

Figure 4. Back-off Time Decision Process

Where, ϕ represents the angle between the line of Xs and the line connecting the node B to the relay node A. Square measure of this striped area in figure 4 is calculated as "fan-shape area – rectangle area". Each square measure is shown as follows.

Half circle:	$\frac{\alpha^2\pi}{2}$
Fan shape:	$\alpha^2\phi$
Rectangle:	$\alpha X_s \sin\phi$

Striped area: $\alpha^2\phi - \alpha X_s \sin\phi$

Ratio of striped area versus half disk:

$$F(Xs) = \frac{2\alpha\phi - 2X_s \sin\phi}{\alpha\pi} \qquad [\phi = \arccos(\frac{Xs}{\alpha})]$$

$$F(Xs) = \frac{2}{\pi}\arccos(\frac{Xs}{\alpha}) - 2X_s \frac{2Xs}{\alpha\pi}\sqrt{1 - \frac{Xs^2}{\alpha^2}} \qquad (3)$$

This ratio *F(Xs)* shows that back-off time in each node is distributed randomly and uniformly by geographical efficiency distance *Xs*. Additionally, the nearer the distance to destination node, the shorter the back-off time becomes. Range of *F(Xs)* is 0~1. Accordingly, back-off time decision function (*BTDF*) is shown as

*BTDF(Xs)=MB*F(Xs)*

where *MB* is Max back-off time defined in system.

In the case where a relay node is in the opposite half disk area away from the destination node (*Xs* is negative), received packet is discarded and further transmission is not performed at this relay node. By repeating these processes at each node, it is possible to configure the route using only geographical effective nodes toward destination node in many cases. Additionally, packet arrival delay can be shortened due to decrease of back-off time by calculating geometric efficiency. Furthermore, it is effective for this system to cancel superfluous transmission of packet from the perspective of the decrease of traffic quantity and power consumption.

3.2. Packet Arrival Rate Improvement for Emergency Packet in Real Situation

As stated in section 2, there is the case that one node is impossible to connect with neighbor node inside the transmission range. This is caused by, for example, node's movement exceeding the transmission range, NLOS, and insufficiency of received signal strength. This degrades packet arrival rate and reliability. It is especially serious for table driven algorithm because of the route construction at one line. Concretely speaking, a route to destination node is constructed but one of the links in the route between one node and another node is disconnected, then it is necessary to retransmit packet using another route. This increases packet arrival delay and degrades throughput. Propagation model of connection probability by distance was shown in figure 2 at section 2.2.

When link disconnection happens, Flooding method, PRCSPR and our proposed method can search other route automatically unlike table driven algorithm. However, degradation of packet arrival rate is inevitable. Especially in the case of medical usage, it is necessary to transmit emergency packets, e.g. health deterioration data. Accordingly, it is necessary to improve packet arrival rate in such propagation situation. In order to improve the reliability of emergency packet transmission, we change multi-hop cancellation process at each node in PRCSPR. Concretely speaking, in the case of receiving the FIRST reserved packet, the cancellation process is not performed, however, in the case of receiving the SECOND reserved packet, the cancellation is performed. In other words, this process is to postpone the cancellation. By performing this postponement process for emergency packet only, packet arrival rate can be improved and packet retransmission process can be reduced. Therefore, packet arrival delay can be improved. However, traffic quantity increases slightly compared to default proposed process.

4. Numerical Analysis

In this section, we analyze our proposed method to comparing with Flooding method, Table driven method, and PRCSPR.

4.1. Simulation Parameters

Simulation parameters are shown in table 1.

Trial number	20000
1 slot time	25[μs]
Packet length	90 slot
DIFS time	2 slot
Max back-off time (MB)	31 slot
Field	500x500[m]
Transmission Range	100[m]
Distance between first node and destination node	400[m]
Propagation model constant ***Cp***	1

Table 1. Simulation Parameters

4.2. Packet Arrival Delay versus number of nodes

In order to confirm improvement of communication efficiency of our method, we analyze packet arrival delay (PAD) time versus the number of nodes existing in the field. It is showed that the smaller the PAD, the more the throughput is improved. In this analysis, packet arrival delay is defined as average the delay value only in the case where the packet arrives at destination node. The result is shown in figure 5.

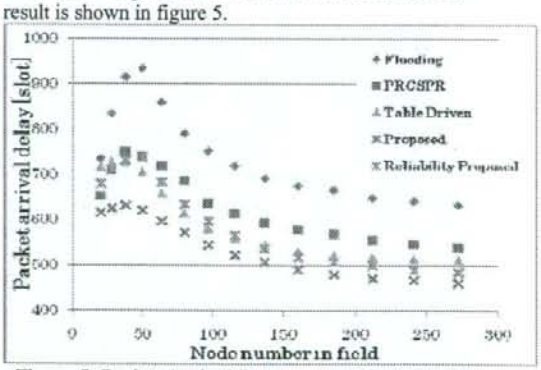

Figure 5. Packet Arrival Delay versus Node Number in Field

Figure 5 shows as follows. Firstly, PAD of flooding method is degraded from the cause of increasing the wait status opportunity of other node's transmission in CSMA/CA protocol. Comparing with flooding method, PRCSPR can reduce the delay due to additional back-off time by canceling redundant transmission in case where repeated transmission by other nodes is sensed. Therefore, PAD can also be reduced. Furthermore, nodes transmit minimal number of packets only in table driven method. Therefore, there is no additional delay by own packet transmission and PAD becomes small. In our proposed method, PAD can be reduced most effectively by shortening back-off time of node in geographical effective position. Finally, the proposed method that enhances reliability (i.e. Reliability Proposed) by retransmission, results in